

1 Finding Shortest Walks in Kuru Kuru Kururin

2 Mickaël Laurent   

3 Charles University, Prague, Czech Republic

4 Maher Mallem   

5 Inria, CNRS, ENS de Lyon, Université Claude Bernard Lyon 1, LIP, UMR 5668, 69342, Lyon cedex
6 07, France

7 — Abstract —

8 This paper serves as a celebration of the twenty-fifth anniversary of *Kuru Kuru Kururin*. Although
9 this video game is presented as a collection of two-dimensional puzzles based on rotation, it naturally
10 invites players to complete its levels as quickly as possible. This has led to a surprisingly rich and
11 challenging playing field to finding foremost temporal walks. In this work, we tackle this problem
12 both in theory and in practice. First, we introduce a model for the game and provide an in-depth
13 complexity analysis. Most notably, we show how each gameplay mechanic independently brings a
14 layer of NP-hardness and/or co-NP-hardness. We also provide a pseudo-polynomial time algorithm
15 for the general problem and identify several cases which can be solved in polynomial time. Along
16 the way, we discuss connections to the more established framework of temporal graphs, both in the
17 point model and the interval model. Then, we propose simple and flexible algorithmic techniques
18 to reduce state space and guide the search, offering trade-offs between precision and computation
19 speed in practice. These techniques were implemented and tested using a full recreation of the game
20 physics and the levels from the original game. We demonstrate the efficiency of our framework in
21 several settings - with or without taking damage, with or without unintended game mechanics -
22 and relate empirical struggles which we encountered in practice to our complexity analysis. Our
23 implementation is open source and fully available online, offering a novel and amusing setting to
24 benchmark shortest path algorithms.

25 **2012 ACM Subject Classification** Theory of computation → Problems, reductions and completeness;
26 Theory of computation → Shortest paths

27 **Keywords and phrases** shortest path, complexity

28 **Digital Object Identifier** 10.4230/LIPIcs.CVIT.2016.23

29 1 Introduction

30 *Kuru Kuru Kururin* is a video game published by Nintendo for the Game Boy Advance in
31 2001. This game is composed of a succession of levels, in which the player (the *helirin*) has
32 to walk through a maze, from the *start area* to (one of the) *ending area(s)*.



33 **Figure 1** The helirin never
34 stops rotating (here, clockwise)

35 **Figure 2** When hitting a
wall, it loses a heart...

Figure 3 ...and is repelled
(both in position and angle)

33 While studying the computational complexity of video games is nothing new (e.g.,
34 see [3, 9, 10] for classic video game series and [8, 17, 23] for pathfinding in video games), this
35 game is unique in that the helirin constantly spins around at a fixed angular speed. The

23:2 Finding Shortest Walks in Kuru Kuru Kururin

36 player cannot control its rotation speed, but can move the helirin up, down, left, right, and
 37 diagonally at three possible speeds (slow, medium, or fast). The helirin initially has three
 38 hearts. When the helirin hits a wall, it loses one heart and gets repelled (both in position
 39 and angle) as shown in Figures 1, 2 and 3. When reaching zero hearts, the level must be
 40 restarted from the start area. The level may contain some healing areas, which restore all
 41 hearts and prevent the helirin from taking damage. The starting area also has this effect.

42 Some additional mechanics are introduced in later levels. For instance, *springs* that
 43 reverse the direction of rotation of the helirin (clockwise / counterclockwise) when hit, or
 44 *moving objects* (pistons and spiked balls) that follow a predefined path and must be avoided
 45 (cf. Figures 4, 5 and 6).



Figure 4 Some moving pistons and springs



Figure 5 The helirin hits a spring...



Figure 6 ...which reverses its rotation direction

46 This paper is organized as follows. In Section 2, we propose a simplified model of the
 47 base gameplay, and extend it with additional mechanics (springs and moving objects). Then,
 48 we study complexity of each variant in Section 3. Section 4 then studies the actual game
 49 implementation and shows how to design an approximate path finding algorithm despite
 50 the gigantic number of states. Finally, in Section 5 we introduce KuruBot, our path-finder
 51 implementation for *Kuru Kuru Kururin*, then we elaborate on how it can be configured to
 52 achieve different goals.

2 Preliminaries

54 ▶ **Definition 1.** \mathbb{N} , \mathbb{Z} , and \mathbb{Q} are respectively defined as the set of positive integers, integers
 55 and rational numbers. \mathbb{Z}^+ and \mathbb{Q}^+ are respectively defined as the set of non-negative integers
 56 and non-negative rational numbers.

2.1 Base Gameplay

58 ▶ **Definition 2.** A *helirin* \mathcal{H} is defined as a tuple $(\ell, \nu_{card}, \nu_{diag}, \omega)$ which represents a
 59 half-length $\ell \in \mathbb{N}$ a cardinal speed $\nu_{card} \in \mathbb{N}$ a diagonal pointwise speed $\nu_{diag} \in \mathbb{N}$ and an
 60 angular speed $\omega\pi$, $\omega \in \mathbb{Q}^+$.

61 ▶ **Definition 3.** A *base helirin state* \mathcal{S} is defined as a tuple (x, y, α, b) representing a
 62 center position $(x, y) \in \mathbb{Z}^2$, an angle $\alpha\pi \in \mathbb{Q}\pi$, $0 \leq \alpha < 1$ and a boolean $b \in \{0, 1\}$ indicating
 63 whether the helirin is turning counterclockwise.

64 We treat angles modulo π . Like in the unit circle, angles are measured from segment
 65 $[(0, 0), (0, 1)]$ and increase as you turn counterclockwise. By default, we assume that a helirin
 66 is turning counterclockwise - i.e., $b = 1$.

67 ▶ **Definition 4.** The *base moveset* \mathcal{M} is $\{\emptyset, N, NE, E, SE, S, SW, W, NW\}$, i.e., a stand-
 68 still and the eight cardinal and diagonal directions “north”, “north-east”, etc..

69 A **base move** is a couple $(\mu, d) \in \mathcal{M} \times \mathbb{N}$ where d is the **duration** of the move.

70 During a move, the helirin is constantly spinning around by an angle $\omega\pi$ (resp. $-\omega\pi$) per
71 time unit if it is turning counterclockwise (resp. clockwise).

72 ► **Definition 5.** A **base helirin walk** $\mathcal{W} = (S_0, t_0, (\mu_1, d_1), \dots, (\mu_k, d_k))$ is a sequence of
73 base moves from an initial state S_0 and time t_0 . The **duration** of walk \mathcal{W} is defined as
74 $d(\mathcal{W}) = d_1 + \dots + d_k$.

75 ► **Definition 6.** Let $s \in \mathbb{N}$. A **tile** is a $s \times s$ square in the plane which can interact with the
76 helirin. The **base tileset** Σ features a **goal tile** kind, which only interacts with the center of
77 the helirin, and **wall tile** kinds, which forbid a polygonal zone within the tile to intersect with
78 any part of the helirin. There are five of them here: the plain square, and the four triangles
79 filling half of the square.

80 A **base tile** is a tuple $(\kappa, s, x, y) \in \Sigma \times \mathbb{N} \times \mathbb{Z} \times \mathbb{Z}$ where κ is the tile kind, s is the side
81 length and (x, y) are the coordinates of the bottom-left corner of the $s \times s$ square.

82 We allow tiles to overlap each other. Plus, like in *Kuru Kuru Kururin*, we consider that
83 goal tiles have priority over wall tiles. In other words, collisions with wall tiles are ignored if
84 the center of the helirin is in a goal tile.

85 ► **Definition 7.** A **base helirin state** \mathcal{S} is said to be **valid** if and only if the helirin does not
86 intersect with a forbidden square of a wall tile. A **base helirin walk** \mathcal{W} is said to be **valid** if
87 and only if all intermediate states during the walk are valid.

88 ► **Definition 8.** Problem **BASEKURURIN**.

89 INPUT: A helirin \mathcal{H} , a set of base tiles $\mathcal{T} = \{(\kappa_1, s_1, x_1, y_1), \dots, (\kappa_N, s_N, x_N, y_N)\}$, a base
90 helirin state S_0 , times $t_0, D \in \mathbb{Z}^+$.

91 QUESTION: Starting from state S_0 and time t_0 , is there a valid base helirin walk to a goal
92 tile of duration at most D ?

93 Let N be the number of tiles. For the sake of simplicity, in the rest of the paper, we
94 assume that we have pre-implemented routines to check whether a given base helirin state is
95 valid in $\mathcal{O}(N)$ time, and whether a given base helirin walk is valid in polynomial time.

96 2.2 Additional Gameplay Mechanics

97 ► **Definition 9.** A segment in the plane has the **mirroring property** if the following behavior
98 occurs. Let q be the denominator of angular speed factor ω . If any part of the helirin would
99 intersect the helirin after a unit-time move, the helirin rotation is reverted back by steps of
100 $1/q$ until it no longer intersects with the spring tile edge - say, after an angle p/q . Then the
101 rotation is reverted back by an additional angle p/q , and the helirin now turns the other way
102 around.

103 A **spring tile** is a tile where exactly one edge of the square has the mirroring property.

104 When **BASEKURURIN** is augmented with spring tiles, four tile kinds are added to base tile-
105 set Σ : one for each choice of edge which has the mirroring property.

106 ► **Definition 10.** A **piston** is defined as a tuple $(s, x, y, \tau, t_{on}, t_{off}, (\mu, d), \nu)$ which represents
107 a square of side length $s \in \mathbb{N}$, the starting coordinates $(x, y) \in \mathbb{Z}^2$ of the bottom-left corner, a
108 time period $\tau \in \mathbb{N}$, a periodic activating time $t_a \in \{0, \dots, \tau - 1\}$, a periodic deactivating time
109 $t_d \in \{0, \dots, \tau - 1\}$, a base move $(\mu, d) \in \mathcal{M} \times \mathbb{N}$ and a (pointwise) speed $\nu \in \mathbb{N}$.

23:4 Finding Shortest Walks in Kuru Kuru Kururin

110 ► **Definition 11.** A *spiked ball* is defined as a tuple $(r, x, y, \tau, t_0, (\mu, d), \nu)$ which represents
 111 a disk of radius $r \in \mathbb{N}$, the starting coordinates $(x, y) \in \mathbb{Z}^2$ of the bottom-left corner of the
 112 square which inscribes the disk outer circle, a time period $\tau \in \mathbb{N}$, a periodic starting time
 113 $t_0 \in \{0, \dots, \tau - 1\}$, a base move $(\mu, d) \in \mathcal{M} \times \mathbb{N}$ and a (pointwise) speed $\nu \in \mathbb{N}$.

114 In the presence of pistons and/or spiked balls, a base helirin walk is valid if and only if,
 115 on top of wall tiles, the helirin never intersects with them during the walk.

116 2.3 Other Problems

117 ► **Definition 12.** Problem *SUBSETSUM*.

118 INPUT: Elements $a_1, \dots, a_n \in \mathbb{N}$, target $B \in \mathbb{N}$.

119 QUESTION: Is there a set $S \subseteq \{1, \dots, n\}$ such that $\sum_{i \in S} a_i = B$?

120 ► **Definition 13.** Let V be a set of vertices. A *timed arc* is a tuple (u, v, t, δ) representing a
 121 directed arc $(u, v) \in V^2$, a departure time $t \in \mathbb{Z}^+$ and a travel time $\delta \in \mathbb{N}$. A *point temporal*
 122 *graph* \mathcal{G} is of the form (V, \mathcal{A}) where \mathcal{A} is a set of timed arcs.

123 An *interval timed arc* is a tuple (u, v, t, t', δ) representing a directed arc $(u, v) \in V^2$,
 124 an earliest and a latest departure time $t, t' \in \mathbb{Z}^+$ and a travel time $\delta \in \mathbb{N}$. An *interval*
 125 *temporal graph* \mathcal{G} is of the form (V, \mathcal{A}) where \mathcal{A} is a set of interval timed arcs.

126 ► **Definition 14.** A *temporal walk* W in a (point or interval) temporal graph $\mathcal{G} = (V, \mathcal{A})$ is a
 127 sequence of timed arcs $((u_1, v_1, t_1, \delta_1), \dots, (u_k, v_k, t_k, \delta_k))$ such that, for all $i \in \{1, \dots, k - 1\}$,
 128 $v_i = u_{i+1}$ and $t_i + \delta_i \leq t_{i+1}$. In the point model, arcs must belong to \mathcal{A} . In the interval model,
 129 for every timed arc $(u_i, v_i, t_i, \delta_i)$ in the walk, there must be an interval timed arc (u, v, t, t', δ)
 130 in \mathcal{A} such that $t \leq t_i \leq t'$. The walk is called *restless* if $t_1 = 0$ and $t_i + \delta_i = t_{i+1}$ for all i .
 131 The *arrival time* of W is $(t_k + \delta_k)$.

132 ► **Definition 15.** Problem *(RESTLESS)FOREMOSTTEMPORALWALK*.

133 INPUT: A (point or interval) temporal graph $\mathcal{G} = (V, \mathcal{A})$, two vertices $u, v \in V$,
 134 a time $D \in \mathbb{Z}^+$.

135 QUESTION: Is there a (restless) temporal walk from u to v with arrival time at most D ?

136 RESTLESSFOREMOSTTEMPORALWALK is in P on point temporal graphs [2], whereas it
 137 is weakly NP-hard on interval temporal graphs [22, 28], even with constant vertex-interval-
 138 membership-width [6]. FOREMOSTTEMPORALWALK is in P with both models [5].

139 3 Computational Complexity

140 In this section, we establish the computational complexity of problem BASEKURURIN. We
 141 start from the original problem, then consider several gameplay mechanics one by one and
 142 study their respective impact on the problem complexity. Omitted proofs are available in
 143 Appendix A.

144 3.1 Base Gameplay

145 First, we show that the base problem is in PSPACE.

146 ► **Theorem 16.** *BASEKURURIN* is in PSPACE.

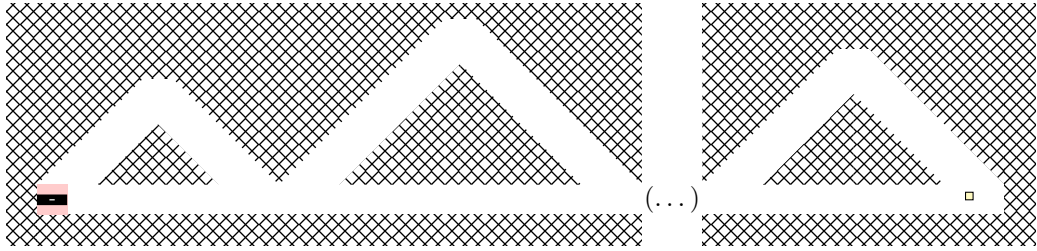
147 Indeed, recall that PSPACE = NPSPACE from Savitch's theorem [25]. So, if there exists a
 148 valid base helirin walk $\mathcal{W} = (\mathcal{S}_0, t_0, (\mu_1, d_1), \dots, (\mu_k, d_k))$, we can find it by guessing moves

¹⁴⁹ (μ_i, d_i) in order, performing them on-the-fly while checking the validity of the corresponding
¹⁵⁰ walk prefixes. We do so while keeping track of the current base helirin state, and of time
¹⁵¹ with a non-negative integer variable, checking that it never goes above D .

¹⁵² Next, we show that the base problem is NP-hard, regardless of the value of the angular
¹⁵³ speed.

¹⁵⁴ ▶ **Theorem 17.** *BASEKURURIN is weakly NP-hard even when $\omega = 0$.*

¹⁵⁵ We reduce from weakly NP-hard problem SUBSETSUM [12]. We take inspiration from the
¹⁵⁶ NP-hardness proof of problem RESTLESSFOREMOSTTEMPORALWALK on interval temporal
¹⁵⁷ graphs by Zeitz [28]. Figure 7 illustrates the created instance of BASEKURURIN. For each
¹⁵⁸ choice of element a_i in SUBSETSUM, we have two branching paths: one where you go east
¹⁵⁹ for $2a_i$ time units, and another where you go north-east from a_i time units, then south-east
¹⁶⁰ for a_i time units. Both paths are then merged. Element a_i is included in the subset if and
¹⁶¹ only if we chose the path going north-east then south-east.



■ **Figure 7** Layout of the NP-hardness reduction of BASEKURURIN. The isolated square at the right represents the single 1×1 goal tile

¹⁶² Note that this reduction would work with any angular speed ω : it purely relies on the
¹⁶³ offset between cardinal and diagonal speed values, which gets magnified over time. As such,
¹⁶⁴ time D needs to be encoded in binary for our reduction to work. In fact, if time D is given
¹⁶⁵ in unary in the input, then BASEKURURIN can be solved in polynomial time.

¹⁶⁶ ▶ **Theorem 18.** *BASEKURURIN is pseudo-polynomial-time solvable.*

¹⁶⁷ We show this by encoding our instance as a point temporal graph with $\mathcal{O}(D^4)$ ver-
¹⁶⁸ tices and $\mathcal{O}(D^5)$ timed arcs. Each accessible center position can be encoded as a tu-
¹⁶⁹ ple $(n_N, n_{NE}, n_E, n_{SE})$ of values in $\{-D, \dots, D\}$ giving a signed number of unit-time base
¹⁷⁰ moves in each direction in order to reach it. And timed arcs are of the form $(u, v, t, 1)$,
¹⁷¹ where u represents a center position accessible at time t and v represents a center position
¹⁷² accessible from u with one of the nine unit-time base moves. If N is the number of tiles
¹⁷³ in our instance I of BASEKURURIN then, in $\mathcal{O}(D^5N)$ time, we can compute all accessible
¹⁷⁴ center positions, including whether they are in a goal tile, and compute an equivalent point
¹⁷⁵ temporal graph \mathcal{G}_I . Then problem FOREMOSTTEMPORALWALK can be solved in linear time
¹⁷⁶ on \mathcal{G}_I to look for a walk from the starting center position to all accessible center positions in
¹⁷⁷ goal zones simultaneously [4].

¹⁷⁸ ▶ **Remark 19.** Conversely, FOREMOSTTEMPORALWALK on point temporal graphs can be
¹⁷⁹ reduced to BASEKURURIN.

¹⁸⁰ Additionally, in the proof of Theorem 17, note that wall tiles were crucial to enforce specific
¹⁸¹ durations for the diagonal base moves which corresponded to the elements in the instance
¹⁸² of SUBSETSUM. If there are no such walls then, for each goal tile, one can compute a base

23:6 Finding Shortest Walks in Kuru Kuru Kururin

183 helirin walk reaching it in minimum duration via an integer linear program with a constant
184 number of variables and constraints. We have eight non-negative integer variables indicating
185 the number of unit-time base moves in each of the eight directions. We aim to minimize
186 their sum while ending the walk in the square goal tile (i.e., with four constraints). Each
187 system can be solved in $\mathcal{O}(1)$ time (e.g., see [1]), so we can solve our problem in $\mathcal{O}(N)$ time.

188 ▶ **Theorem 20.** *BASEKURURIN with no wall tiles is polynomial-time solvable.*

189 3.2 Base Gameplay with Diagonal Speed Restrictions

190 In this subsection, we restrict the value of diagonal pointwise speed ν_{diag} such that we cannot
191 reuse the trick used to prove the NP-hardness of BASEKURURIN in Theorem 17. In particular,
192 if $\nu_{diag} \in \{0, \nu_{card}\}$, then one can no longer create a position offset other than a multiple
193 of ν_{card} . In fact, the graph of accessible center positions with unit-time move neighborhood is
194 a grid graph, with a four-neighborhood if $\nu_{diag} = 0$ and an eight-neighborhood if $\nu_{diag} = \nu_{card}$.
195 With such neighborhoods, it is not hard to see that the triangle inequality is satisfied. As
196 such, if additionally the helirin does not spin around, then the instance of BASEKURURIN
197 can be easily turned into such grid graphs and solved efficiently. E.g., by using the visibility
198 graph induced by the corners of the wall tiles [18, 21, 27], we can solve this particular case
199 in $\mathcal{O}(N^2)$ time.

200 ▶ **Theorem 21.** *BASEKURURIN with $\nu_{diag} \in \{0, \nu_{card}\}$ and $\omega = 0$ is polynomial-time solvable.*

201 However, if the helirin is allowed to spin around, then we believe that our problem is
202 again unlikely to be polynomial-time solvable.

203 ▶ **Conjecture 22.** *BASEKURURIN is weakly co-NP-hard even when $\nu_{diag} \in \{0, \nu_{card}\}$.*

204 This would show that both speed offset and rotation independently make our problem
205 difficult.

206 3.3 Base Gameplay with Spring Tiles

207 If spring tiles are available, then the reduction of Theorem 17 can be adapted by using the
208 mirroring property to create an angle offset in the rotation of the helirin between branching
209 paths. Arbitrary angle offsets can be obtained within constant duration, so this reduction
210 does not require time D to be given in binary in the input.

211 ▶ **Theorem 23.** *BASEKURURIN augmented with spring tiles is weakly NP-hard even when
212 $\nu_{diag} \in \{0, \nu_{card}\}$ and time D is given in unary.*

213 Still, the algorithm from Theorem 18 can be adapted if, on top of time D , the denomina-
214 tor q_ω of angular speed factor ω is given in unary in the input. Then the number of vertices
215 in the equivalent point temporal graph is in $\mathcal{O}(D^4 q_\omega)$.

216 ▶ **Theorem 24.** *BASEKURURIN augmented with spring tiles is pseudo-polynomial-time
217 solvable.*

218 3.4 Base Gameplay With Pistons and Spiked Balls

219 If pistons or spiked balls are available, then the algorithm from Theorem 18 can be easily
220 adapted with minor time overhead. Indeed, these elements are time-indexed so, at each time,
221 their location can easily be determined and taken into account when computing the set of
222 accessible center positions.

223 ▶ **Theorem 25.** *BASEKURURIN augmented with pistons and spiked balls is pseudo-polynomial-time solvable.*

225 However, having these moving elements makes our problem difficult independently from
226 all previous gameplay mechanics - namely speed offset, rotation and spring tiles.

227 ▶ **Theorem 26.** *BASEKURURIN augmented with pistons or spiked balls is weakly NP-hard and weakly co-NP-hard even when $\nu_{diag} \in \{0, \nu_{card}\}$, $\omega = 0$ and half-length ℓ , cardinal speed ν_{card} and tile sizes s_i are given in unary.*

230 Indeed, note that spiked balls with standstill base moves and pistons with unit-time base
231 moves essentially act as periodic on/off switches, with periods written in binary. So, these
232 periods can be given exponential values within logarithmic working space [7, 24], which is
233 the key ingredient in our reductions. For instance, this allows us to test all valuations of a
234 boolean formula - and thus encode both SAT and DNF-TAUTOLEGY.

235 ▶ **Remark 27.** (RESTLESS)FOREMOSTTEMPORALWALK on interval temporal graphs can be
236 reduced to BASEKURURIN augmented with spiked balls.

237 ▶ **Remark 28.** Finally, since the problem is both NP-hard and co-NP-hard, it is unlikely that
238 it belongs to either class. Indeed if, e.g., it belonged to NP, then co-NP-complete problem
239 DNF-TAUTOLEGY would also belong to NP. This would mean that NP = co-NP, which
240 would imply a collapse of the Polynomial Hierarchy to the second level [26].

241 4 Algorithmic Techniques

242 In this section, we provide algorithmic techniques aimed at tackling real instances of *Kuru*
243 *Kuru Kururin*.

244 4.1 State Space

245 Recall that a base helirin state features a center position (x, y) , an angle α , and a boolean b
246 indicating whether the helirin is turning counterclockwise. In the actual implementation of
247 *Kuru Kuru Kururin*, these are stored as follows:

248 **56 bits** position: 32 bits for x, 32 bits for y, with the 4 most-significant bits unused in
249 practice. The 16 less-significant bits are sub-pixel precision—the position in pixels can be
250 retrieved by only reading the 16 most-significant bits,
251 **16 bits** angle (evenly captures the $[0, 2\pi[$ interval),
252 **1 bit** rotation direction (clockwise / counterclockwise).

253 In addition, when colliding with walls, the helirin gets repelled¹. This mechanism is
254 modeled by adding the following components to the state:

255 **40 bits** bump speed: 32 bits for x, 32 bits for y, with the 12 most-significant bits unused in
256 practice. Bump speed is added to the helirin when hitting a wall and decreases with time,
257 **12 bits** rotation speed: 16 bits, with the 4 most-significant bits unused in practice. Rotation
258 speed is added to the helirin when hitting a wall, and stabilizes towards the base rotation
259 speed with time.

¹ For the sake of simplicity, in Section 2 we did not model this knock-back mechanism, and instead focused on a variant where collisions with walls are not allowed. Though it is clear that it would make the base problem more difficult, at least by considering angle offsets in the helirin rotation similarly to springs.

23:8 Finding Shortest Walks in Kuru Kuru Kururin

260 This amounts to a total of 125 bits, i.e., roughly $6 \cdot 10^{37}$ states, which would be too
261 massive to explore exhaustively. Encoding base helirin states with a temporal graph as in
262 Theorem 18 would help in shorter levels, though not nearly enough. Indeed, *Kuru Kuru*
263 *Kururin* level durations typically range from a couple seconds to a minute, so consider a
264 level which can be finished in ten seconds. Since the game runs at roughly sixty frames per
265 second, this would still amount to $600^4 \cdot 2^{52} \simeq 6 \cdot 10^{26}$ states. Consequently, looking for
266 optimal resolution by exhaustive search seems impractical. In response, we propose a custom
267 implementation of the A* algorithm, which we detail in the next section.

268 Note that, for some levels and applications, even more components must be added to the
269 state (e.g., hearts and invulnerability frames for non-damageless gameplay as in Section 5.2,
270 or the position of the moving objects for maps that contain some). More information about
271 the state and how it evolves can be found in the notes of our first *tool-assisted speedrun* [15].

272 4.2 Custom A* Algorithm

273 In order to find short walks in spite of the very large state graph, we propose a custom
274 implementation of the A* search algorithm. First, a heuristic function is computed by
275 computing distance of every point to the target in an approximated variant of the problem
276 (we call this heuristic function the “cost map”, Section 4.2.1). Then, this heuristic function
277 is used to guide a custom A* search algorithm (Section 4.2.2).

278 4.2.1 Cost map

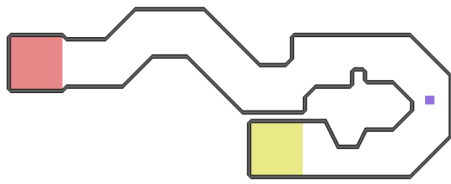
279 The heuristic function used to guide the A* search is computed using a Dijkstra algorithm that
280 starts at the end of the level and computes, for each state, its distance to the end. However,
281 the state space used for this heuristic function is harshly approximated: it assimilates the
282 helirin with a point (thus making all angle-related state irrelevant), and ignores movements
283 due to the collision with walls (thus eliminating the state related to bump speed). Depending
284 on the application, walls can either be considered impassable, or passable under certain
285 conditions and at a certain cost (cf. Section 5). In this context, as walls are aligned on pixels,
286 the precision of the position can be reduced to the pixel unit, thus saving 32 bits of state.
287 The state is thus only composed of the x and y position of 12 bits each, yielding 2^{24} states
288 (which is perfectly fine to explore exhaustively).

289 This yields a cost map that associates to each pixel of the map a distance to the end of
290 the level (or to a custom target). It is then used to guide the A* algorithm for the resolution
291 with the full state. This cost map is not necessarily an under-approximation of the real cost,
292 as considering the helirin as being punctual allows turning closer to the walls. Consequently,
293 we cannot guarantee that the A* search that find an optimal path. Also note that the cost
294 map can be multiplied by a constant factor to parametrize the influence it has on the search:
295 a factor higher than 1 will often explore fewer states, resulting in a faster resolution but a
296 solution that is less optimal.

297 4.2.2 Reducing the search space

298 The algorithm we use to find a minimal path is based on the A* search algorithm [11] with
299 the heuristic function h induced by our cost map:

- 300 1. Let Q be a priority queue. For each starting state s , the pair $(s, 0)$ is added to Q with
301 priority $h(s)$.
- 302 2. The pair (s, l) of minimum priority is extracted from Q .



■ **Figure 8** Map of the first level:
Grasslands 1 (start area, ending area)



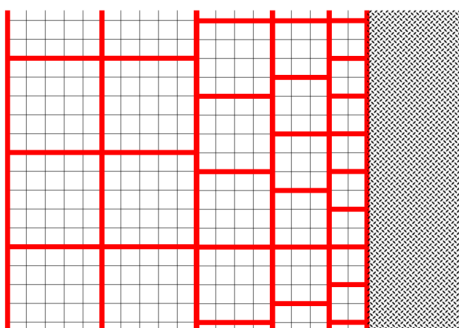
■ **Figure 9** Associated cost map
(unpassable walls)

303 ■ If this is a final state, then the algorithm terminates: a path of length l has been found.
304 ■ Otherwise, the successors of s are computed, and for each such successor s' , the pair
305 $(s', l + 1)$ is added to Q with priority $l + 1 + h(s)$. This step is then repeated.

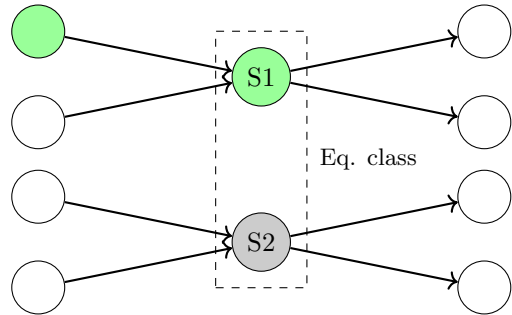
306 In practice, this algorithm does not terminate even for simple levels. Thus, we implemented
307 two main strategies for reducing the search space.

308 **Equivalence classes**

309 A first way to reduce the search space is to define equivalence classes regrouping states that
310 are *sufficiently similar*. This is done by defining a state normalization function $n(s)$ that
311 truncates some of the state components to the desired precision (that can be configured
312 depending on the application, cf. Section 5). Two states s_1 and s_2 are in the same equivalence
313 class if and only if $n(s_1) = n(s_2)$.



■ **Figure 10** Equivalence classes for
position (smaller near the wall on the right)



■ **Figure 11** Path finding: node S2 is
disabled because S1 has been reached first

314 The searching algorithm is then amended to never explore two states of the same
315 equivalence class. For that, it maintains a set of normalized states S : when a state s is
316 extracted from the priority queue Q , $n(s)$ is added to S – if it was already present, then s is
317 removed from Q without exploring it. This is illustrated by Figure 11.

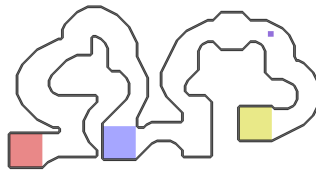
318 Also note that we may want a dynamic resolution for the search: states that are close to
319 a wall may benefit from a higher resolution because of the complex dynamic of collisions (in
320 particular when solving for unrestricted gameplay, cf. Section 5.2). Thus, our normalization
321 function n implements adaptive precision: the closer to a wall a state is, the fewer digits are
322 truncated. This is illustrated in Figure 10.

23:10 Finding Shortest Walks in Kuru Kuru Kururin

323 Piecewise solving

324 Another way to reduce the search space is to perform a piecewise solving: *checkpoints* are
 325 inserted in the level, fragmenting the map into segments that are solved successively. Once
 326 a checkpoint has been reached, no other path to this checkpoint will be explored, and the
 327 search for a path to the next checkpoint starts.

328 This strategy can be achieved in two ways. First, it can be achieved by manually
 329 performing multiple searches: a first one from the starting state to an arbitrary area
 330 (checkpoint 1), then another search from the resulting state to another area (checkpoint 2),
 331 and so on. Second, it can be achieved in an automated way by modifying the cost map
 332 so that reaching a checkpoint area induces a huge decrease of the estimated cost. This is
 333 illustrated in Figures 12, 13 and 14 where checkpoints have been added on healing areas
 334 (these are good spots to insert checkpoints as they offer a great mobility: when the helirin is
 335 in a healing area, it can easily change its angle by hitting a wall without taking damage).



■ **Figure 12** Map (start area, healing area, ending area)



■ **Figure 13** Cost map (no checkpoint)

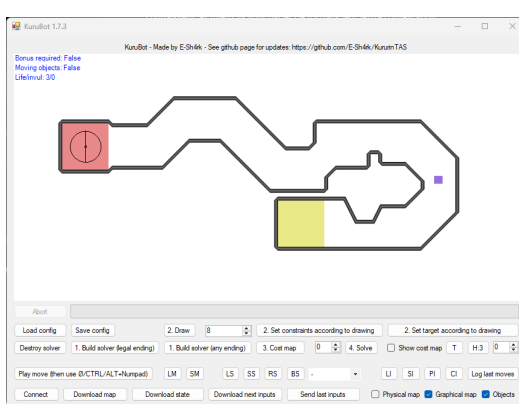


■ **Figure 14** Cost map (with checkpoint)

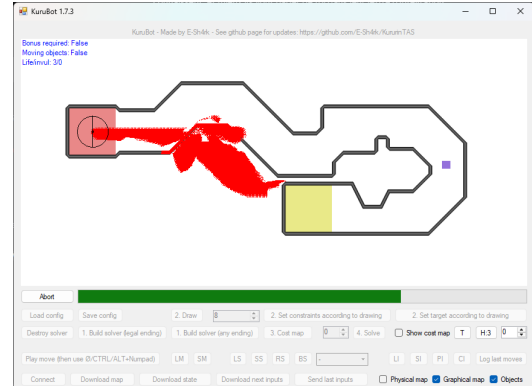
336 5 Applications

337 5.1 Implementation: KuruBot

338 The exact physics of the game Kuru Kuru Kururin as well as the path finding algorithm
 339 described in Section 4 have been implemented in KuruBot [14], a C# application of about
 340 4000 lines of code. It can also communicate with the emulator BizHawk in order to retrieve
 341 the current map and state from a live session, find a path, and play it on the emulator.
 342 Several configurations can be loaded to achieve different goals that we present in this section.



■ **Figure 15** Interface of KuruBot



■ **Figure 16** KuruBot while searching for a path

343 5.2 Categories

344 Levels can be solved with different constraints (“*categories*”). The main categories are
 345 presented below. Solving each category requires using an adapted configuration for KuruBot,
 346 which are summarized in Figure 17.

Category	Cost map	Resolution (base, near walls)	Checkpoints
Damageless	No wall crossing	2 px, 2 px	Automated, at healing areas
Regular intended	No wall crossing	2 px, 1 px	Automated, at healing areas
Regular unrestricted	Wall crossing if hearts > 1	1 px, 1/8 px	Manual, short segments

347 **Figure 17** Configuration adapted for each category

347 Damageless completion

348 The damageless completion category consists in finishing every level without taking any
 349 damage. Note that hitting a wall may still be permitted if the helirin is in a healing zone
 350 (thus, the bump speed and rotation speed components of the state cannot be neglected). A
 351 *tool-assisted speedrun* of this category made using KuruBot is available on TASVideos.org [16].

352 Regular completion, intended gameplay

353 For regular completion, the helirin is allowed to hit walls, which can be used to walk through
 354 narrow spaces, to have a boost due to the speed bump, and to change the angle of the
 355 helirin. When hitting a wall outside a healing area, the helirin loses a heart and becomes
 356 invulnerable for 20 frames. Thus, the following bits must be added to our state:

357 **2 bits** remaining hearts (max: 3),
 358 **5 bits** invulnerability frames (max: 20).

359 Regular completion, unrestricted gameplay

360 The unrestricted category allows exploiting the physics of the game, in particular the way
 361 collisions are handled, to break through walls. However, such manipulations are only possible
 362 for some wall placements, and require a very precise combination of position, angle, and
 363 bump speed to be performed. Consequently, for this category, the resolution of the solver
 364 (cf. Section 4.2.2) must be increased (in particular the resolution near walls).

365 The cost map computation is also modified: crossing walls is allowed, but at a constant
 366 cost to account for the number of frames it takes to cross a wall in average (e.g. 10 frames),
 367 and only if the helirin has at least 2 hearts (otherwise, hitting a wall will lose the level).
 368 Consequently, two cost maps must be computed: one that will be used when the helirin has
 369 at least 2 hearts left, and one when it has only one heart (cf. Figures 18 and 19). Positions
 370 that are inside walls also get a constant cost reduction to account for the fact that these are
 371 advantageous areas inside which the helirin should stay as long as possible (in particular, the
 372 helirin can move faster when it is inside a wall). A *tool-assisted speedrun* of this category
 373 made using KuruBot is available on TASVideos.org [20].

23:12 Finding Shortest Walks in Kuru Kuru Kururin

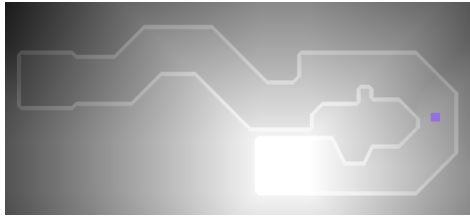


Figure 18 Unrestricted gameplay cost map (with extra hearts)

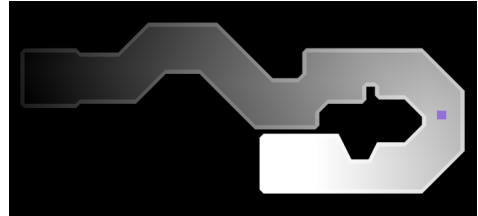


Figure 19 Unrestricted gameplay cost map (no extra heart)

374 Other incentives

375 We may want to search for solutions that minimize measures other than the total number of
376 frames. For instance, minimizing the number of input changes (i.e. the number of times a
377 button must be pressed or released) can also be of interest in order to find *humanly-viable*
378 ways to cross a wall for speedrunners. Such paths have already been found by using KuruBot
379 with an adapted configuration [19].

380 6 Conclusion

381 In this work, we presented an algorithmic and complexity study of *Kuru Kuru Kururin*,
382 a puzzle-action game whose distinctive mechanics naturally give rise to rich shortest-walk
383 problems. By formalizing the game’s behavior and progressively extending the model with
384 additional mechanics, we revealed how each gameplay element (rotation, speed asymmetries,
385 spring tiles, moving objects, etc.) introduces its own source of computational hardness. Our
386 results show that even the base problem is weakly NP-hard, and that various mechanics
387 independently raise the difficulty to NP-hard or even co-NP-hard levels. Despite these
388 hardness results, when time or mechanical constraints are restricted, several variants admit
389 pseudo-polynomial-time or even polynomial-time algorithms.

390 In the second part of this article, focusing this time on approximate resolution, we
391 introduced practical algorithmic techniques, including a state-space reduction strategy and a
392 custom A* search guided by approximate cost maps, that enable efficient solving of real game
393 levels despite an astronomically large underlying state space. Finally, we implemented these
394 ideas in KuruBot, a full physics-accurate path-finding framework capable of exploring a wide
395 variety of gameplay settings. Overall, this work bridges complexity theory, temporal graph
396 reasoning, and game physics modeling, showing how a charming 2001 Game Boy Advance
397 title can serve as a surprisingly deep computational playground.

398 Going forward, in the short term we plan to benchmark the performance of our path
399 finding algorithm in the presence of the different elements introduced in the complexity
400 analysis. Using a level editor that we created [13], we plan to generate multiple levels, each
401 focusing on a specific mechanic: base gameplay without diagonal moves, base gameplay
402 with diagonal moves, springs, moving objects, etc. The performance on these benchmark
403 levels will then be evaluated using a specific configuration of KuruBot, and compared to the
404 conclusions of our complexity analysis. Moreover, such levels could also serve as an amusing
405 playing field to compare state-of-the-art pathfinding algorithms.

406 Finally, in the future, our complexity analysis could be extended to model the whole
407 game, including knock-back, the life system and healing areas, as well as the sequels *Kururin*
408 *Paradise* and *Kururin Squash!*, hidden gems which were only released in Japan and feature
409 even more unique game mechanics to explore.

410

 References

411 1 Nina Amenta, Jesús A De Loera, and Pablo Soberón. Helly’s theorem: new variations and
412 applications. *Algebraic and geometric methods in discrete mathematics*, 685:55–95, 2017.

413 2 Matthias Bentert, Anne-Sophie Himmel, André Nichterlein, and Rolf Niedermeier. Efficient
414 computation of optimal temporal walks under waiting-time constraints. *Applied Network
415 Science*, 5(1):73, 2020.

416 3 Jeffrey Bosboom, Josh Brunner, Michael J. Coulombe, Erik D. Demaine, Dylan H. Hendrickson,
417 Jayson Lynch, and Elle Najt. The legend of zelda: The complexity of mechanics. *CoRR*,
418 abs/2203.17167, 2022. URL: <https://doi.org/10.48550/arXiv.2203.17167>, arXiv:2203.
419 17167, doi:10.48550/ARXIV.2203.17167.

420 4 Filippo Brunelli and Laurent Viennot. Computing temporal reachability under waiting-
421 time constraints in linear time. In David Doty and Paul Spirakis, editors, *2nd Symposium on
422 Algorithmic Foundations of Dynamic Networks (SAND 2023)*, volume 257 of *Leibniz
423 International Proceedings in Informatics (LIPIcs)*, pages 4:1–4:11, Dagstuhl, Germany, 2023.
424 Schloss Dagstuhl – Leibniz-Zentrum für Informatik. doi:10.4230/LIPIcs.SAND.2023.4.

425 5 Binh-Minh Bui-Xuan, Afonso Ferreira, and Aubin Jarry. Computing shortest, fastest, and
426 foremost journeys in dynamic networks. *International Journal of Foundations of Computer
427 Science*, 14(02):267–285, 2003. doi:10.1142/S0129054103001728.

428 6 Justine Cauvi and Laurent Viennot. Parameterized restless temporal path. In Artur Jeż and
429 Jan Otop, editors, *Fundamentals of Computation Theory*, pages 82–93, Cham, 2026. Springer
430 Nature Switzerland. doi:10.1007/978-3-032-04700-7_7.

431 7 Yiping Cheng. Space-efficient Karatsuba multiplication for multi-precision integers. *arXiv
432 preprint arXiv:1605.06760*, 2016. URL: <https://arxiv.org/abs/1605.06760>.

433 8 Xiao Cui and Hao Shi. Direction oriented pathfinding in video games. *International Journal
434 of Artificial Intelligence & Applications*, 2(4):1, 2011.

435 9 Erik D. Demaine, Holden Hall, Hayashi Layers, Ricardo Ruiz, and Naveen Venkat. You
436 can’t solve these super mario bros. levels: Undecidable mario games. *Theoretical Computer
437 Science*, 1060:115549, 2026. URL: <https://www.sciencedirect.com/science/article/pii/S0304397525004876>, doi:https://doi.org/10.1016/j.tcs.2025.115549.

438 10 MIT Hardness Group, Erik D. Demaine, Holden Hall, and Jeffery Li. Tetris with
439 few piece types. *Theoretical Computer Science*, 1059:115581, 2026. URL: <https://www.sciencedirect.com/science/article/pii/S0304397525005195>, doi:https://doi.org/10.
440 1016/j.tcs.2025.115581.

441 11 Peter E. Hart, Nils J. Nilsson, and Bertram Raphael. A formal basis for the heuristic
442 determination of minimum cost paths. *IEEE Transactions on Systems Science and Cybernetics*,
443 4(2):100–107, 1968. doi:10.1109/TSSC.1968.300136.

444 12 Richard M. Karp. *Reducibility among Combinatorial Problems*, pages 85–103. Springer US,
445 Boston, MA, 1972. doi:10.1007/978-1-4684-2001-2_9.

446 13 Mickaël “E-Sh4rk” Laurent and contributors. Repository of ROM-hacking tools for the GBA
447 Kururin games, 2021. URL: <https://github.com/E-Sh4rk/KuruTools>.

448 14 Mickaël “E-Sh4rk” Laurent and contributors. Repository of KuruBot and other TAS tools,
449 2024. URL: <https://github.com/E-Sh4rk/KururinTAS>.

450 15 Mickaël “E-Sh4rk” Laurent and Maher “mohoc” Mallem. Author notes of the tool-assisted
451 speedrun of Kuru Kuru Kururin on TASVideos.org, 2019. URL: <https://tasvideos.org/6314S>.

452 16 Mickaël “E-Sh4rk” Laurent and Maher “mohoc” Mallem. Tool-assisted speedrun of Kuru
453 Kuru Kururin - baseline category, 2019. URL: <https://tasvideos.org/3933M>.

454 17 Sharmad Rajnish Lawande, Graceline Jasmine, Jani Anbarasi, and Lila Iznita Izhar. A
455 systematic review and analysis of intelligence-based pathfinding algorithms in the field of video
456 games. *Applied Sciences*, 12(11), 2022. URL: <https://www.mdpi.com/2076-3417/12/11/5499>,
457 doi:10.3390/app12115499.

461 18 Tomás Lozano-Pérez and Michael A Wesley. An algorithm for planning collision-free paths
462 among polyhedral obstacles. *Communications of the ACM*, 22(10):560–570, 1979.

463 19 Maher “mohoc” Mallem. Kuru Kuru Kururin speedrunning guide - pause frame document,
464 2024. URL: https://www.speedrun.com/kuru_kuru_kururin/resources/ecdzb.

465 20 Maher “mohoc” Mallem. Tool-assisted speedrun of Kuru Kuru Kururin - 100% category, 2024.
466 URL: <https://tasvideos.org/6116M>.

467 21 Marcell Missura, Daniel D. Lee, and Maren Bennewitz. Minimal construct: Efficient shortest
468 path finding for mobile robots in polygonal maps. In *2018 IEEE/RSJ International Conference
469 on Intelligent Robots and Systems (IROS)*, pages 7918–7923, 2018. doi:10.1109/IROS.2018.
470 8594124.

471 22 Ariel Orda and Raphael Rom. Traveling without waiting in time-dependent networks is NP-
472 hard. Technical report, Dept. Electrical Engineering, Technion - Israel Institute of Technology,
473 Haifa, Israel 32000, 1989.

474 23 Sara Lutami Pardede, Fadel Ramli Athallah, Yahya Nur Huda, and Fikri Dzulfiqar Zain.
475 A review of pathfinding in game development. *CEPAT] Journal of Computer Engineering:
476 Progress, Application and Technology*, 1(01):47, 2022.

477 24 Daniel S. Roche. Space- and time-efficient polynomial multiplication. In *Proceedings of the
478 2009 International Symposium on Symbolic and Algebraic Computation*, ISSAC ’09, page
479 295–302, New York, NY, USA, 2009. Association for Computing Machinery. doi:10.1145/
480 1576702.1576743.

481 25 Walter J. Savitch. Relationships between nondeterministic and deterministic tape complex-
482 ities. *Journal of Computer and System Sciences*, 4(2):177–192, 1970. URL: <https://www.sciencedirect.com/science/article/pii/S00220007080006X>, doi:[https://doi.org/10.1016/S0022-0000\(70\)80006-X](https://doi.org/10.1016/S0022-0000(70)80006-X).

485 26 Larry J. Stockmeyer. The polynomial-time hierarchy. *Theoretical Computer Science*, 3(1):1–22,
486 1976. doi:[https://doi.org/10.1016/0304-3975\(76\)90061-X](https://doi.org/10.1016/0304-3975(76)90061-X).

487 27 Tansel Uras, Sven Koenig, and Carlos Hernandez. Subgoal graphs for optimal pathfinding
488 in eight-neighbor grids. *Proceedings of the International Conference on Automated Planning
489 and Scheduling*, 23(1):224–232, Jun. 2013. URL: <https://ojs.aaai.org/index.php/ICAPS/article/view/13568>, doi:10.1609/icaps.v23i1.13568.

491 28 Tim Zeitz. NP-hardness of shortest path problems in networks with non-FIFO time-dependent
492 travel times. *Information Processing Letters*, 179:106287, 2023. doi:<https://doi.org/10.1016/j.ipl.2022.106287>.

494 **A Complexity Proofs**

495 **A.1 Theorem 17**

496 **Proof.** We reduce from weakly NP-hard problem SUBSETSUM [12]. Let a_1, \dots, a_n be the
497 elements and let B be the target. Let $A = \sum_{1 \leq i \leq n} a_i$ and $L = 2A + 1$.

498 We propose the following instance of BASEKURURIN. We set the helirin properties to
499 $(\ell, \nu_{card}, \nu_{diag}, \omega) = (L, 2L, 2L - 1, 0)$. We set $D = 2A + n - 1$ and $\mathcal{S}_0 = (L, L, 0, 1)$. We
500 set wall tiles to form the instance illustrated in Figure 7. For each choice of element a_i in
501 SUBSETSUM, we have two branching paths: one, which we call $P_{i,0}$, where you go east for
502 $2a_i$ time units, and another, which we call $P_{i,1}$, where you go north-east for a_i time units,
503 then south-east for a_i time units. Both paths are then merged. Finally, there is a single 1×1
504 goal tile at position $((2D + 1)L - 2B, L)$.

505 If our instance of SUBSETSUM has a solution $S \subseteq \{1, \dots, n\}$, we propose base helirin
506 walk \mathcal{W} where, for all $i \in \{1, \dots, n\}$, we take path $P_{i,1}$ if $i \in S$ and path $P_{i,0}$ otherwise.
507 This walk is valid and ends at position $((2D + 1)L - 2(\sum_{i \in S} a_i), L) = ((2D + 1)L - 2B, L)$.
508 Conversely, if we have a valid base helirin walk \mathcal{W} , by our choice for speed values ν_{card}, ν_{diag}

509 and time D , only the east, north-east and south-east directions can be used. Therefore,
 510 according to the position of wall tiles, the underlying path from base helirin walk \mathcal{W} is
 511 necessarily of the form $P_{i,j_1} \cdots P_{n,j_n}$ with $j_i \in \{0, 1\}$ for all i . We propose $S = \{i \in$
 512 $\{1, \dots, n\} | j_i = 1\}$. Then, because \mathcal{W} is valid and ends at position $((2D + 1)L - 2B, L)$, we
 513 have: $2B = 2(\sum_{i \in S} a_i)$. \blacktriangleleft

514 A.2 Remark 19

515 The main idea is to keep track of time with the rotation angle. By taking a large enough
 516 half-length ℓ of the helirin compared to the denominator q_ω of angular speed factor ω , we
 517 can discriminate between angles which are multiples of π/q_ω , e.g., by setting wall tiles in
 518 a similar way as in the proof of Theorem 23. Using this trick, having the time span of the
 519 input temporal graph fit within a single half-rotation, we can replicate the layout of the
 520 input temporal graph, and only make the start and the end of the representation of each
 521 timed arc available at specific angles - and thus at specific times.

522 A.3 Theorem 20

523 **Proof.** We have eight non-negative integer variables $(x_\mu)_{\mu \in \mathcal{M} \setminus \{\emptyset\}}$, representing the time
 524 spent going in each of the eight directions. For each goal tile of side length $s^{(i)}$ and bottom-left
 525 corner coordinates $(x^{(i)}, y^{(i)})$, we propose the following integer linear program:

$$\begin{aligned} \text{minimize} \quad & \sum_{\mu \in \mathcal{M} \setminus \{\emptyset\}} x_\mu \\ \text{subject to} \quad & \nu_{\text{card}}(x_E - x_W) + \nu_{\text{diag}}(x_{NE} + x_{SE} - x_{NW} - x_{SW}) \geq x^{(i)}, \\ & \nu_{\text{card}}(x_E - x_W) + \nu_{\text{diag}}(x_{NE} + x_{SE} - x_{NW} - x_{SW}) \leq x^{(i)} + s^{(i)}, \\ & \nu_{\text{card}}(x_N - x_S) + \nu_{\text{diag}}(x_{NE} + x_{NW} - x_{SE} - x_{SW}) \geq y^{(i)}, \\ & \nu_{\text{card}}(x_N - x_S) + \nu_{\text{diag}}(x_{NE} + x_{NW} - x_{SE} - x_{SW}) \leq y^{(i)} + s^{(i)}, \\ & x_\mu \in \mathbb{Z}^+, \mu \in \mathcal{M} \setminus \{\emptyset\}. \end{aligned}$$

527 This ensures that we land on the goal tile as soon as possible. We have a constant number
 528 of variables and constraints, so the system can be solved in $\mathcal{O}(1)$ time (e.g., see [1]). Thus, by
 529 taking the minimum over all goal tiles, we can conclude whether, starting from base helirin
 530 state \mathcal{S}_0 , there is a valid base helirin walk to a goal tile with duration at most D . \blacktriangleleft

531 A.4 Theorem 23

532 **Proof.** (Sketch.) We reduce from weakly NP-hard problem SUBSETSUM [12]. Let a_1, \dots, a_n
 533 be the elements and let B be the target. Let $A = \sum_{1 \leq i \leq n} a_i$ and $L = 16(A + 2n + 1)$.

534 We propose a similar reduction to the proof of Theorem 17, except we rely on rotation
 535 angle offsets instead of position offsets. We set $D = 6n + 1$, $q_\omega = L/2$ and $p_\omega = 1 + q_\omega/8$. We
 536 set the helirin properties to $(\ell, \nu_{\text{card}}, \nu_{\text{diag}}, \omega) = (L, 2L, 0, p_\omega/q_\omega)$ and we set $\mathcal{S}_0 = (L, L, 0, 1)$.
 537 We set wall tiles to form the instance illustrated in Figure 20. For each choice of element a_i
 538 in SUBSETSUM, we have two branching paths: one, which we call $P_{i,0}$, where you go south,
 539 then east for 2 time units, then north, and another, which we call $P_{i,1}$, where you go north,
 540 then east for 2 time units, then south. Both paths are then merged. Plus, there is a single
 541 $2L \times 2L$ goal tile at position $((4n + 1)2L, 0)$.

542 Now, let $\mathcal{P} = \{0, \dots, q_\omega/2\}$. Given $p \in \mathcal{P}$, let (x_p, y_p) be the coordinates of the right
 543 extremity of the helirin at angle $p\pi/q_\omega$. Since $L > 2q_\omega/\sqrt{2}$, function $(p \mapsto (x_p, y_p))$ is
 544 injective over \mathcal{P} , and sequences $(x_p)_{p \in \mathcal{P}}$ and $(y_p)_{p \in \mathcal{P}}$ are respectively non-decreasing and

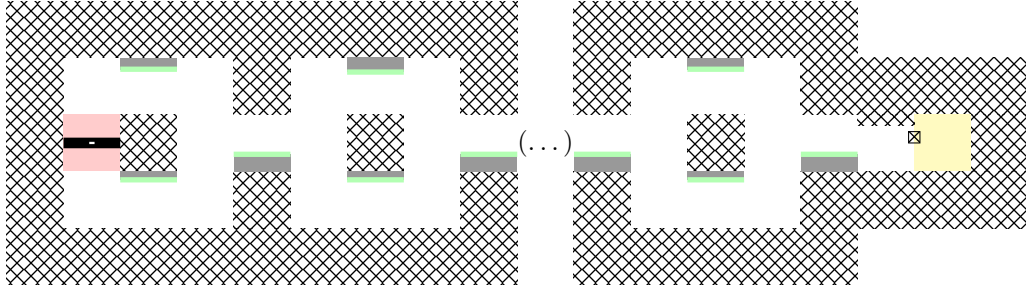


Figure 20 Layout of the NP-hardness reduction with spring tiles. The isolated square at the left of the goal tile is a wall tile which is part of the angle check gadget, which only allows for angle $(B + 2n)\pi/8L$.

545 non-increasing. Plus, for each $p \in \mathcal{P}$, couple (x_p, y_p) is merely a rational approximation of
 546 the cosine and sine of angle $p\pi/q_\omega$, and thus can be computed in polynomial time.

547 Knowing this, we can use these values to position our spring tiles accordingly. In bottom
 548 paths $P_{i,0}$, we rely on numerator ($p = q_\omega/4 + 1$) to align the edges with the mirroring property.
 549 In bottom paths $P_{i,1}$, we rely on numerator ($p = q_\omega/4 + 1 - a_i$) instead. And, once both
 550 paths are merged, we rely on numerator ($p = -q_\omega/8$). Finally, right before the goal tile, we
 551 set two wall tiles in order to block positions (x_p, y_p) for every $p \in \mathcal{P} \setminus \{B + 2n\}$. Then the
 552 correspondence between valid base helirin walks and solutions of the SUBSETSUM instance
 553 unfolds similarly to the proof of Theorem 17. Finally, one can easily adapt the reduction to
 554 case $\nu_{diag} = \nu_{card}$.

555

◀

556 A.5 Theorem 26

557 We detail proofs which make use of spiked balls with standstill base moves. In both of them,
 558 we set the helirin properties to $(\ell, \nu_{card}, \nu_{diag}, \omega) = (1, 2, 0, 0)$ and base helirin state \mathcal{S}_0 to
 559 $(x, y, \alpha, b) = (1, 1, 0, 0)$. Plus, all spiked balls will have radius 1, $\mu = \emptyset$ in their base move,
 560 and $\nu = 1$. So, all relevant elements will be set along a grid of 2×2 squares.

561 NP-hardness

562 **Proof.** We reduce from 3-SAT. Let $\varphi = \bigwedge_{1 \leq i \leq m} (l_{i,1} \vee l_{i,2} \vee l_{i,3})$ be a 3-CNF formula with
 563 m clauses and n variables, w.l.o.g. with exactly three literals per clause. We encode the
 564 formula as an obstacle course going from left to right. Figure 21 represents the base layout,
 565 which can be easily obtained with square wall tiles. Each vertical layer represents a clause
 566 and has three available ways, each associated to a literal in this clause. And we set a single
 567 goal tile of side length 2 at $(x, y) = (4m + 4, 0)$. Then, going from the start area (in red) to
 568 the goal tile (in yellow) with no wait takes time at most $T = 6m + 6$.

569 The plan is to dedicate time T for each of the 2^n valuations of the variables to give them
 570 a chance to reach the goal tile from the start, which will correspond to making φ true. First,
 571 we only allow the helirin to leave the start area at periodic times ($1 \bmod T$). We do so
 572 with a spiked ball at $(x, y) = (2, 0)$ with $\tau = T, t_0 = 2$ and $d = T - 1$. Plus, once the helirin
 573 leaves the start area, we force it to reach the goal tile by the end of the time period. We do
 574 so by setting spiked balls for every $2 \leq i \leq 2m + 2$ and $0 \leq j \leq 4$ at $(x, y) = (2i, 2j)$ with
 575 $\tau = T, t_0 = 0$ and $d = 1$.

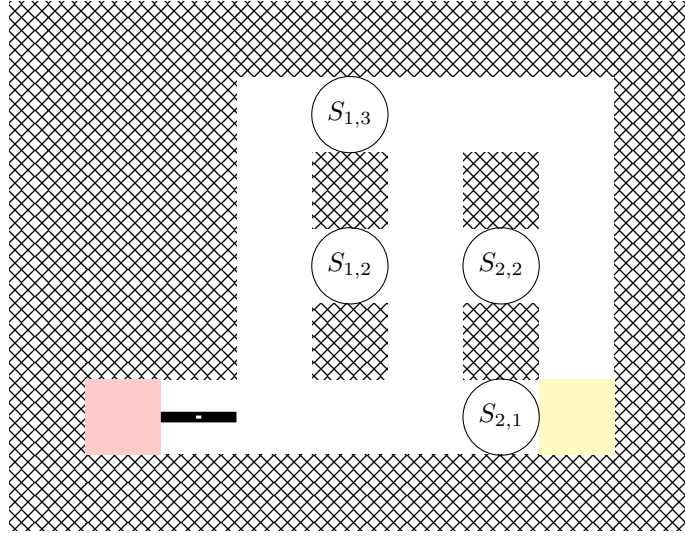


Figure 21 Layout of the NP-hardness reduction with spiked balls, illustrated with input formula $\varphi = (x_1 \vee x_2 \vee x_4) \wedge (x_2 \vee x_3 \vee \neg x_4)$. We are at time $\Delta + 1$, i.e., about to check valuation $(x_4, x_3, x_2, x_1) = (0, 0, 0, 1)$, which makes φ true by choosing literals x_1 then $\neg x_4$.

Now, for $1 \leq k \leq n$ we tie variable x_k to spiked balls of time period $\tau = T2^k$. More precisely, given $1 \leq i \leq m$ and $1 \leq j \leq 3$, we set a spiked ball $S_{i,j}$ at $x = 4i + 2$ and $y = 4j - 4$, with move duration $d = T2^{k-1}$ and:

- if $l_{i,j} = x_k$ is a positive literal: $\tau = T2^k, t_0 = 0, d = T2^{k-1}$,
- if $l_{i,j} = \neg x_k$ is a negative literal: $\tau = T2^k, t_0 = d = T2^{k-1}$.

In other words, spiked balls tied to literal x_k (resp. $\neg x_k$) block their respective path during periodic times $(0, \dots, T2^{k-1} - 1 \bmod T2^k)$ (resp. $(T2^{k-1}, \dots, T2^k - 1 \bmod T2^k)$).

We now piece everything together. Let us consider valuations (x_n, \dots, x_1) by lexicographic order. Given $0 \leq h \leq 2^n - 1$, let v_h be the h^{th} valuation by lexicographic order. Then, v_h matches with the binary representation of h from the right (e.g., the value of x_1 in v_h is the last digit). Knowing this, consider time units $Th, \dots, T(h+1) - 1$. During them, by the definition of spiked balls $S_{i,j}$, the latter block their respective path if and only if:

- $l_{i,j} = x_k$ and the $(k-1)^{\text{th}}$ digit of h from the right is 0, or
- $l_{i,j} = \neg x_k$ and the $(k-1)^{\text{th}}$ digit of h from the right is 1.

Thus the missing spiked balls $S_{i,j}$ exactly correspond to the literals which are made true by valuation v_h . As a result, starting from time Th , we can reach the goal tile by time $T(h+1)$ if and only if v_h makes φ true. Finally, we have that φ is satisfiable if and only if, starting from base helirin state \mathcal{S}_0 , there is a base helirin walk reaching the goal tile by time $D = T2^n$. ◀

594 co-NP-hardness

Proof. We reduce from 3-DNF-TAUTOLEGY. Let $\varphi = \bigvee_{1 \leq i \leq m} (l_{i,1} \wedge l_{i,2} \wedge l_{i,3})$ be a 3-DNF formula with m conjunctions and n variables, again w.l.o.g. with exactly three literals per conjunction. We encode the formula as an obstacle course going from left to right with parallel subpaths, one per conjunction in φ . Then, instead of reaching a goal tile, we allow the helirin to loop back to the start area. Figure 22 represents the base layout, which can be easily obtained with square wall tiles.

The plan is to dedicate time T for each of the 2^n valuations of the variables, this time forcing each one of them to loop through the structure, essentially choosing a subpath - i.e.,

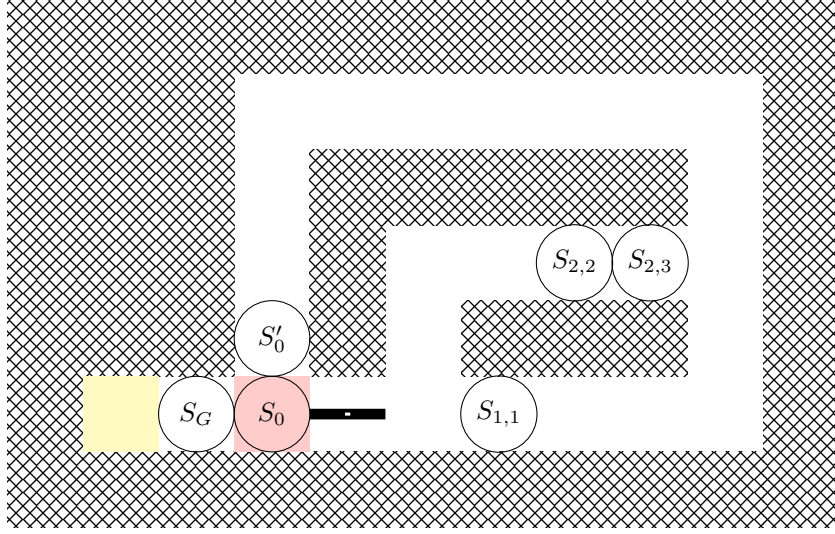


Figure 22 Layout of the co-NP-hardness reduction with spiked balls, illustrated with input formula $\varphi = (\neg x_1 \wedge \neg x_2 \wedge \neg x_4) \vee (x_1 \wedge x_3 \wedge x_4)$. We are at time $T + 1$, i.e., about to check valuation $(x_4, x_3, x_2, x_1) = (0, 0, 0, 1)$, which makes φ false.

603 a conjunction in φ . First, we set $T = 4m + 6$, $D = T2^n + 2$ and set a spiked ball S_G at
 604 $(x, y) = (-2, 0)$ with $\tau = D, t_0 = 0$ and $d = D - 2$. Then, at the beginning of each period,
 605 we force the helirin to leave the start area and head to the right. We do so with two more
 606 spiked balls:

- 607 ■ S_0 at $(x, y) = (0, 0)$ with $\tau = T, t_0 = 1$ and $d = T - 1$,
- 608 ■ S'_0 at $(x, y) = (0, 2)$ with $\tau = T, t_0 = 0$ and $d = 2$.

609 Plus, we force the helirin to reach the end of our loop by the end of each time period. We do
 610 so by setting spiked balls for every couple $(i, j) \in \{0, \dots, 6\} \times \{0, \dots, 2m + 1\} \setminus \{(0, 0), (0, 1)\}$
 611 at $(x, y) = (2i, 2j)$ with $\tau = T, t_0 = T - 1$ and $d = 2$. Then, other than time $D - 1$, the
 612 helirin is necessarily at positions $(1, 3), (1, 1), (3, 1)$ at respective periodic times $(T - 1, 0, 1$
 613 $\bmod T)$.

614 Now, for $1 \leq k \leq n$ we tie variable x_k to spiked balls of time period $\tau = T2^k$. More
 615 precisely, given $1 \leq i \leq m$ and $1 \leq j \leq 3$, we set a spiked ball $S_{i,j}$ at $x = 2j + 4$ and
 616 $y = 4i - 4$, with move duration $d = T2^{k-1}$ and:

- 617 ■ if $l_{i,j} = x_k$ is a positive literal: $\tau = T2^k, t_0 = 0, d = T2^{k-1}$,
- 618 ■ if $l_{i,j} = \neg x_k$ is a negative literal: $\tau = T2^k, t_0 = d = T2^{k-1}$.

619 Then, we have the same correspondence as in the previous proof between spiked ball
 620 appearances and valuations considered by lexicographic order. So, starting from time Th with
 621 $0 \leq h \leq 2^n - 1$, we can reach position $(1, 3)$ by time $T(h + 1)$ if and only if the h^{th} valuation
 622 v_h by lexicographic order makes φ true. Thus, we have that φ is a tautology if and only
 623 if, starting from base helirin state S_0 , there is a base helirin walk reaching the goal tile by
 624 time D . \blacktriangleleft

625 Finally, it is clear that both reductions also work if $\nu_{\text{diag}} = \nu_{\text{card}}$. Furthermore, the role
 626 of spiked balls with standstill base moves can be easily achieved using pistons with unit-time
 627 moves. Indeed, given such a spiked ball $(1, x, y, \tau, t_0, (\emptyset, d), 1)$, it blocks the square delimited
 628 by cells (x, y) and $(x + 2, y + 2)$ in periodic times $(t_0, \dots, t_0 + d - 1 \bmod \tau)$. So, e.g., we can
 629 define piston $(2, x, -2, \tau, t_0, t_0 + d, (N, 1), y + 2)$ to achieve the same result - i.e., when it is

630 inactive it is completely out of the way, and when it is active it blocks the square delimited
631 by cells (x, y) and $(x + 2, y + 2)$.

632 **A.6 Remark 27**

633 Instead of using rotation angles and wall tiles to keep track of time like in Appendix A.2,
634 similarly to the proofs of Theorem 26, we use spiked balls with standstill base moves to set
635 intervals of time at which each edge in the underlying static graph is available. Furthermore,
636 we use moving spiked balls along the representation of each edge in order to dictate exactly
637 the travel time of the helirin along this edge. Not only does this allow us to encode interval
638 temporal graphs, it can also be used to restrict the waiting time of the helirin at each vertex.